Unitary Description of the Jaynes-Cummings Model with Fractional Time: Photon Statistics

Thiago T. Tsutsui, Danilo Cius, Antonio S. M. de Castro e Fabiano M. Andrade

***Abstract*— Recently, a unitary model for the fractional-time Jaynes-Cummings model was proposed. In this work, we deepen the understanding of the model by analyzing its photon statistics, considering an initial coherent state. Depending on the value of the fractional order α, various interesting phenomena are affected, such as sub-Poissonian statistics, squeezing and cat states for the cavity mode. The case where $\alpha = 0.50$ results in periodic squeezing and the formation of cat states. The latter aspect indicates similarities with the two-photon standard Jaynes-Cummings model.**

***Keywords*— Jaynes-Cummings model, Fractional time Schrödinger equation, Time-dependent Dyson map, Photon Statistics.**

I. Introduction

Over the past few decades, theoretical efforts have increasingly focused on broadening the framework of standard quantum mechanics. For instance, one direction involves the use of fractional-order differential operators to construct quantum models capable of capturing nonlocal or anomalous quantum effects [1]. The memory effects associated with this approach enable applications in the context of quantum information, as demonstrated by Zu and coworkers [2].

In parallel, the Jaynes–Cummings (JC) model [3] serves as a fundamental system for studying light–matter interaction in quantum optics, describing the coupling between a two-level atom and a quantized cavity mode. Furthermore, the model has been applied in quantum information processing and quantum computation [4].

The blending of fractional time dynamics with the JC model in the fractional time JC (FTJC) opens new avenues for exploring the behavior of quantized light.

The connection between these two formalisms is outlined by the time fractional Schrödinger equation (TFSE), proposed by Naber [5], considering a Wick rotation of time, $t \to -it/\hbar$.

Thiago T. Tsutsui, Programa de Pós-Graduação em Ciências/Física, Universidade Estadual de Ponta Grossa, Ponta Grossa-PR, e-mail: takajitsutsui@gmail.com; Danilo Cius, Instituto de Física, Universidade de São Paulo, São Paulo-SP, e-mail: danilocius@gmail.com; Antonio S. M. de Castro, Departamento de Física e Programa de Pós-Graduação em Ciências/Física, Universidade Estadual de Ponta Grossa, Ponta Grossa-PR, e-mail: asmcastro@uepg.br; Fabiano M. Andrade, Departamento de Matemática e Estatística, Programa de Pós-Graduação em Ciências/Física, Universidade Estadual de Ponta Grossa, Ponta Grossa-PR e Departamento de Física, Universidade Federal do Paraná, Curitiba-PR, e-mail: fmandrade@uepg.br. This work was partially supported by Coordenação de Aperfeiçoamento de Pessoal de Nível Superior (CAPES, Finance Code 001), Conselho Nacional de Desenvolvimento Científico e Tecnológico (CNPq) and Instituto Nacional de Ciência e Tecnologia de Informação Quântica (INCT-IQ). D.C. acknowledges funding from Instituto Serrapilheira and the PRPI–USP through the Programa de Estímulo à Supervisão de Pós-Doutorandos por Jovens Pesquisadores. F.M.A. acknowledges support from CNPq under Grant No. 313124/2023-0.

In this formulation, the standard time derivative is substituted by the Caputo fractional derivative. Accordingly, TFSE takes the form of

$$i^{\alpha}\, {}_0^{\mathrm{C}}\mathcal{D}_t^{\alpha} \left|\Psi_\alpha(t)\right\rangle = \hat{H}_\alpha \left|\Psi_\alpha(t)\right\rangle, \tag{1}$$

where $\hat{H}_\alpha$ denotes the fractional Hamiltonian operator, while ${}_0^{\mathrm{C}}\mathcal{D}_t^{\alpha}$ stands for the Caputo fractional derivative operator, defined as

$${}_0^{\mathrm{C}}\mathcal{D}_t^{\alpha}(\cdot) = \frac{1}{\Gamma(1-\alpha)} \int_0^t d\tau (t-\tau)^{-\alpha} \frac{d}{d\tau}(\cdot), \tag{2}$$

where $\alpha \in (0, 1]$, and $\Gamma(\cdot)$ denotes the well-known Gamma function. It is noteworthy that the standard Schrödinger equation is recovered in the limit $\alpha \to 1$. Here we consider all variables to be dimensionless.

Remarkably, the TFSE leads to non-unitary time-evolution, presenting a challenge within standard quantum mechanics. Recently, a unitary description of the FTJC was proposed [6], based on the formalism established in Ref. [7]. In this work, we further develop the understanding of this approach to the FTJC model by examining the photon statistics of the quantum light state.

II. Unitary Framework

The TFSE, Eq. (1), significantly modifies the behavior of systems dynamics typically described by the standard Schrödinger equation. In this sense, the application of the Caputo derivative effectively introduces memory effects into the time evolution. Additionally, the time evolution described by Eq. (1) does not conserve the norm of the state vector with respect to the standard inner product, rendering the evolution non-unitary.

To address this, recent studies have proposed embedding the dynamics in a time-dependent non-Hermitian framework [9]. This involves introducing a Dyson map – an invertible, time-dependent operator $\hat{\eta}_\alpha(t)$ – that transforms the non-unitary state $|\Psi_\alpha(t)\rangle$ into a unitarily evolving state $|\psi_\alpha(t)\rangle$:

$$\left|\psi_\alpha(t)\right\rangle = \hat{\eta}_\alpha(t) \left|\Psi_\alpha(t)\right\rangle. \tag{3}$$

Assuming that the states $|\psi_\alpha(t)\rangle$ and $|\Psi_\alpha(t)\rangle$ evolve under the time-evolution operators $\hat{u}_\alpha(t)$ (unitary) and $\hat{U}_\alpha(t)$ (non-unitary), respectively, they can be connected through the relation:

$$\hat{u}_\alpha(t) = \hat{\eta}_\alpha(t)\hat{U}_\alpha(t)\hat{\eta}_\alpha^{-1}(0). \tag{4}$$

Thus, by employing the time-dependent Dyson map, unitarity can be restored in the time evolution, allowing for a conventional interpretation of the FTJC dynamics.

III. The Jaynes-Cummings Model

The JC model [3] is paradigmatic in quantum optics, depicting the quantum dynamics of the interaction between two-level atom and a quantized cavity mode. Assuming atom-field resonance and employing the interaction picture, the JC Hamiltonian is given by

$$\hat{H}_\alpha = \hbar_\alpha \mu_\alpha (\hat{\sigma}_+ \hat{a} + \hat{\sigma}_- \hat{a}^\dagger). \tag{5}$$

The atomic degrees of freedom are described using the Pauli raising and lowering operators ($\hat{\sigma}_\pm$), whereas the quantized cavity field is characterized by the bosonic annihilation and creation operators ($\hat{a}$ and $\hat{a}^\dagger$). The atomic states consist of the excited state ($|e\rangle$) and the ground state ($|g\rangle$), while the Fock states ($|n\rangle$) denote the discrete excitations of the cavity mode.

The JC Hamiltonian also commutes with the total excitation number operator, $\hat{N}_E = \hat{a}^\dagger \hat{a} + \hat{\sigma}_z/2$, which allows the Hamiltonian to be partitioned into 2×2 blocks, along with a single 1×1 block corresponding to the ground state $|g, 0\rangle$. As a result, the system dynamics are confined to a two-dimensional subspace spanned by the basis states $\{|e, n\rangle, |g, n+1\rangle\}$ [4].

For time-independent Hamiltonians evolving under the TFSE, the time evolution operator is written as

$$\hat{U}_\alpha(t) = E_\alpha \left(\frac{i^{-\alpha} \hat{H}_\alpha t^\alpha}{\hbar_\alpha} \right), \tag{6}$$

where $E_\alpha(x)$ represents the one parameter Mittag-Leffler function [1]. The block-diagonal structure of the JC model results in a 2×2 blocks $\hat{U}_\alpha^{(n)}(t)$ acting on each subspace. They are given by

$$\hat{U}_\alpha^{(n)}(t) = \begin{bmatrix} \mathcal{C}_\alpha^{(n)}(t) & i^{-\alpha}\mathcal{S}_\alpha^{(n)}(t) \\ i^{-\alpha}\mathcal{S}_\alpha^{(n)}(t) & \mathcal{C}_\alpha^{(n)}(t) \end{bmatrix}. \tag{7}$$

Here, the complex functions $\mathcal{C}_\alpha^{(n)}(t)$ and $\mathcal{S}_\alpha^{(n)}(t)$ take the form

$$\mathcal{C}_\alpha^{(n)}(t) = \frac{E_\alpha(i^{-\alpha}\mu_\alpha^{(n)} t^\alpha) + E_\alpha(-i^{-\alpha}\mu_\alpha^{(n)} t^\alpha)}{2}, \tag{8a}$$

$$\mathcal{S}_\alpha^{(n)}(t) = \frac{E_\alpha(i^{-\alpha}\mu_\alpha^{(n)} t^\alpha) - E_\alpha(-i^{-\alpha}\mu_\alpha^{(n)} t^\alpha)}{2i^{-\alpha}}. \tag{8b}$$

To obtain a unitary evolution in the FTJC model, we follow the map introduced in Ref. [6]. In accordance with the algebraic structure of the JC model, the map is Hermitian, explicitly time-dependent, and exhibits a block-diagonal structure. The Dyson map that acts on the two-dimensional subspace is given by

$$\hat{\eta}_\alpha^{(n)}(t) = e^{\kappa_\alpha^{(n)}(t)} e^{\lambda_\alpha^{(n)}(t)\hat{\sigma}_+} e^{\ln \Lambda_\alpha^{(n)}(t)\hat{\sigma}_z/2} e^{\left[\lambda_\alpha^{(n)}(t)\right]^* \hat{\sigma}_-}, \tag{9}$$

where we assume $\lambda_\alpha^{(n)}(t) \in \mathbb{C}$ and $\Lambda_\alpha^{(n)}(t), \kappa_\alpha^{(n)}(t) \in \mathbb{R}$, with the additional condition $\Lambda_\alpha^{(n)}(t) > 0$. As a consequence of Eqs. (4) and (9), the operator $\hat{u}_\alpha(t)$ can also be decomposed into 2×2 blocks, denoted by $\hat{u}_\alpha^{(n)}(t)$.

Assuming that $\hat{u}_\alpha(t)$ is unitary, each block $\hat{u}_\alpha^{(n)}(t)$ must accordingly belong to the Lie group $U(2)$ and can be expressed in the general matrix form

$$\hat{u}_\alpha^{(n)}(t) = e^{i\delta_\alpha^{(n)}(t)} \begin{bmatrix} \varpi_{\alpha,+}^{(n)}(t) & \varpi_{\alpha,-}^{(n)}(t) \\ -[\varpi_{\alpha,-}^{(n)}(t)]^* & [\varpi_{\alpha,+}^{(n)}(t)]^* \end{bmatrix}, \tag{10}$$

with

$$\delta_\alpha^{(n)}(t) = \frac{1}{2}\mathrm{Im}[\ln D_\alpha^{(n)}(t)], \tag{11a}$$

$$\varpi_{\alpha,\pm}^{(n)}(t) = \pm e^{i\delta_\alpha^{(n)}(t)} [\nu_{\alpha,\mp}^{(n)}(t)]^*, \tag{11b}$$

The function $D_\alpha^{(n)}(t)$ appearing in Eq. (11a) is given by $D_\alpha^{(n)}(t) = [\mathcal{C}_\alpha^{(n)}(t)]^2 - (-1)^{-\alpha}[\mathcal{S}_\alpha^{(n)}(t)]^2$. For notational simplicity, we henceforth omit the explicit time dependence and introduce the quantities $\nu_{\alpha,\pm}^{(n)}$ in Eq. (11b) as

$$\nu_{\alpha,\pm}^{(n)} = \pm \frac{e^{\kappa_\alpha^{(n)} - \kappa_\alpha^{(n)}(0)}}{\sqrt{\Lambda_\alpha^{(n)}\Lambda_\alpha^{(n)}(0)}} \left[\zeta_{\alpha,\pm}^{(n)} + (\lambda_\alpha^{(n)})^* \xi_{\alpha,\pm}^{(n)} \right], \tag{12}$$

where $\zeta_{\alpha,\pm}^{(n)}$ and $\xi_{\alpha,\pm}^{(n)}$ are given by

$$\zeta_{\alpha,+}^{(n)} = i^{-\alpha}\mathcal{S}_\alpha^{(n)} - [\lambda_\alpha^{(n)}(0)]^* \mathcal{C}_\alpha^{(n)}, \tag{13a}$$

$$\zeta_{\alpha,-}^{(n)} = i^{-\alpha}\lambda_\alpha^{(n)}(0)\mathcal{S}_\alpha^{(n)} - \chi_\alpha^{(n)}(0)\mathcal{C}_\alpha^{(n)}, \tag{13b}$$

$$\xi_{\alpha,+}^{(n)} = \mathcal{C}_\alpha^{(n)} - i^{-\alpha}[\lambda_\alpha^{(n)}(0)]^* \mathcal{S}_\alpha^{(n)}, \tag{13c}$$

$$\xi_{\alpha,-}^{(n)} = \lambda_\alpha^{(n)}(0)\mathcal{C}_\alpha^{(n)} - i^{-\alpha}\chi_\alpha^{(n)}(0)\mathcal{S}_\alpha^{(n)}. \tag{13d}$$

Furthermore, for $\hat{u}_\alpha^{(n)}$ to characterize a unitary operator, the parameters of the time-dependent Dyson map must satisfy the following structure:

$$\kappa_\alpha^{(n)} = \kappa_\alpha^{(n)}(0) - \frac{1}{2}\mathrm{Re}[\ln D_\alpha^{(n)}], \tag{14a}$$

$$\chi_\alpha^{(n)} = \frac{|\zeta_{\alpha,+}^{(n)}|^2 + |\zeta_{\alpha,-}^{(n)}|^2 + \Lambda_\alpha^{(n)}(0) e^{\mathrm{Re}[\ln D_\alpha^{(n)}]}}{|\xi_{\alpha,+}^{(n)}|^2 + |\xi_{\alpha,-}^{(n)}|^2 + \Lambda_\alpha^{(n)}(0) e^{\mathrm{Re}[\ln D_\alpha^{(n)}]}}, \tag{14b}$$

$$\lambda_\alpha^{(n)} = \frac{-\left[\xi_{\alpha,+}^{(n)}[\zeta_{\alpha,+}^{(n)}]^* + \xi_{\alpha,-}^{(n)}[\zeta_{\alpha,-}^{(n)}]^*\right]}{|\xi_{\alpha,+}^{(n)}|^2 + |\xi_{\alpha,-}^{(n)}|^2 + \Lambda_\alpha^{(n)}(0) e^{\mathrm{Re}[\ln D_\alpha^{(n)}]}}, \tag{14c}$$

where the time-dependent Dyson map parameter is given by $\Lambda_\alpha^{(n)} = \chi_\alpha^{(n)} - |\lambda_\alpha^{(n)}|^2$, under the assumption that $\Lambda_\alpha^{(n)}$ remains positive. This implies the condition $\chi_\alpha^{(n)} > |\lambda_\alpha^{(n)}|^2$. It is worth noting that the coefficients of the unitary operator $\hat{u}_\alpha^{(n)}$ rely exclusively on the parameters defining the fractional time evolution operator and the initial conditions of the time-dependent Dyson map. With the operator $\hat{u}_\alpha^{(n)}$ at hand, the unitary dynamics of the system can be determined for any chosen initial state.

IV. Photon Statistics

In this section, we analyze the photon statistics of the FTJC evolved state within a unitary framework. Assuming the cavity begins in a coherent state ($|\beta\rangle$) and the atom in the excited state ($|e\rangle$), the initial state of the system is given by

$$|\psi_\alpha(0)\rangle = |e, \beta\rangle = e^{-\frac{|\beta|^2}{2}} \sum_{n=0}^{\infty} \frac{\beta^n}{\sqrt{n!}} |e, n\rangle. \tag{15}$$

The system evolves according to $|\psi_\alpha(t)\rangle = \hat{u}_\alpha(t)|\psi_\alpha(0)\rangle$, resulting in

$$|\psi_\alpha(t)\rangle = \sum_{n=0}^{\infty} \left[A_{e,n}^\alpha(t)|e, n\rangle + A_{g,n}^\alpha(t)|g, n+1\rangle \right], \tag{16}$$

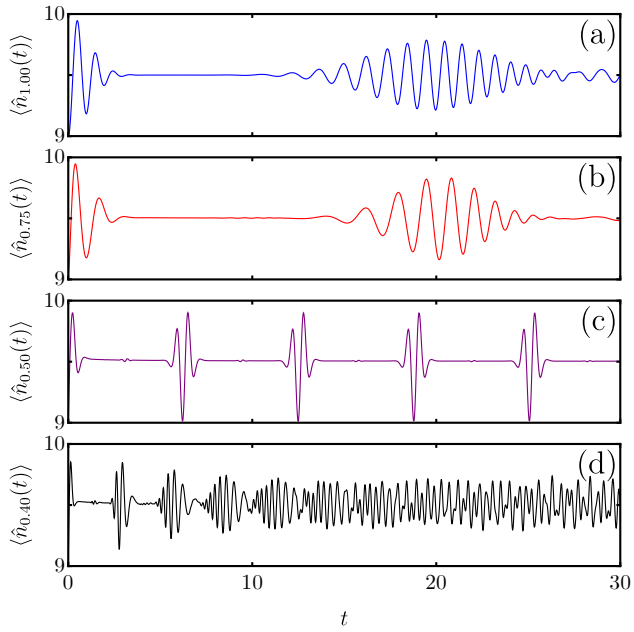

Fig. 1. The average photon number for the FTJC model, for different values of α: $\alpha = 1.00$ (a), $\alpha = 0.75$ (b), $\alpha = 0.50$ (c) and $\alpha = 0.40$ (d).

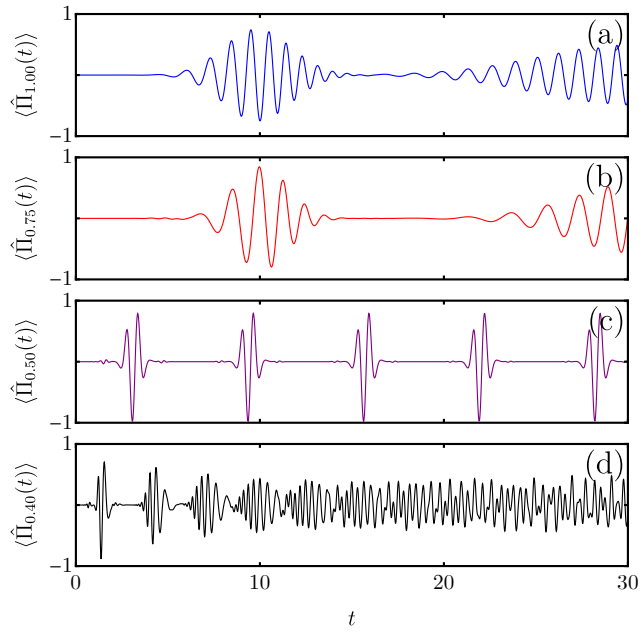

Fig. 2. The average parity for the FTJC model, for different values of α: $\alpha = 1.00$ (a), $\alpha = 0.75$ (b), $\alpha = 0.50$ (c) and $\alpha = 0.40$ (d).

with $A^{\alpha}_{e,n}(t)$ and $A^{\alpha}_{g,n}(t)$ denoting probability amplitudes. With Eq. (10), we obtain the specific form of the probability amplitudes, which we leave implicit.

For the subsequent simulations, we set $\beta = 3$ and $\mu_\alpha = 1$, with the initial Dyson map parameters fixed as $\kappa_\alpha(0) = \lambda_\alpha(0) = 0$ and $\Lambda_\alpha(0) = 1$.

A. Average Photon Number

The number operator is defined as $\hat{n}_\alpha = \hat{a}^\dagger \hat{a}$. We denote its expectation value at time t by $\langle \hat{n}_\alpha(t) \rangle$. Initially, this value reflects the field intensity, yielding $\langle \hat{n}_\alpha(0) \rangle = |\beta|^2$. The behavior of $\langle \hat{n}_\alpha(t) \rangle$ is presented in Fig. 1, for different fractional orders.

In panel (a), for $\alpha = 1.00$, we recover the well-known pattern of collapses and revivals [4]. Panel (b), corresponding to $\alpha = 0.75$, exhibits a qualitatively similar behavior, though the evolution proceeds more slowly. In contrast, panel (c), where $\alpha = 0.50$, reveals a markedly different dynamics, characterized by periodicity. At times $t = q\pi$ with $q = 0, 2, 4, \ldots$, we observe oscillations in the expectation value. More generally, for $\alpha < 0.50$, as illustrated in panel (d) with $\alpha = 0.40$, the dynamics becomes increasingly irregular.

B. Parity

Following the analysis in Ref. [10], we examine the parity properties of the field using the parity operator $\hat{\Pi}_\alpha = (-1)^{\hat{n}_\alpha}$, which indicates whether the photon number is even or odd. Fig. 2 displays the expectation value of the parity operator in the FTJC model.

In panel (a), corresponding to $\alpha = 1.00$, we observe the typical behavior: the photon-number parity oscillates precisely when the average photon number remains nearly constant (Fig. 1(a)), i.e., around the midpoint of the collapse interval. This effect arises from the interference between counter-rotating components of the field as the system evolves in time. In particular, for $\alpha = 0.50$, shown in panel (c), the parity oscillations occur periodically at times $t = m\pi$, with $m = 1, 3, 5, \ldots$.

C. Mandel Parameter

The Q-Mandel parameter [4] is a photon statistics tool employed to study the type of distribution associated with a given state of light, according to the expected value and uncertainty, denoted by $\Delta^2 \hat{n}_\alpha(t)$, of the number operator. Governed by

$$Q_\alpha(t) = \frac{\Delta^2 \hat{n}_\alpha(t)}{\langle \hat{n}_\alpha(t) \rangle} - 1, \tag{17}$$

the parameter classifies the light source as Poissonian ($Q_\alpha(t) = 0$), super-Poissonian ($Q_\alpha(t) > 0$) and sub-Poissonian ($Q_\alpha(t) < 0$).

Fig. 3 presents the Q-Mandel parameter for the FTJC model. For $\alpha = 1.00$, a pattern bearing resemblance to the collapse and revival phenomenon is recovered, modulating the parameter between super-Poissonian and sub-Poissonian regimes during both the initial oscillations and the revival phases. For $\alpha = 0.50$, the system once again displays periodicity. Compared to the other cases, there are more pronounced quiescent intervals in which $Q_{0.50}(t)$ stabilizes at a negative value. Oscillations reappear when the corresponding expectation value of the number operator varies, (Fig. 1(c)). Furthermore, the Q-Mandel parameter attains lower values than in the other cases, signaling a higher degree of non-classicality in the field statistics.

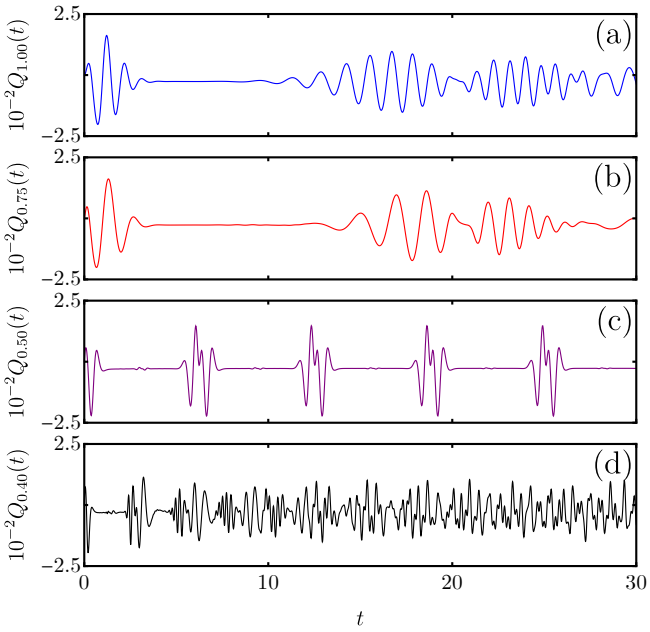

Fig. 3. The Q-Mandel parameter for the FTJC model, for different values of α: $\alpha = 1.00$ (a), $\alpha = 0.75$ (b), $\alpha = 0.50$ (c) and $\alpha = 0.40$ (d).

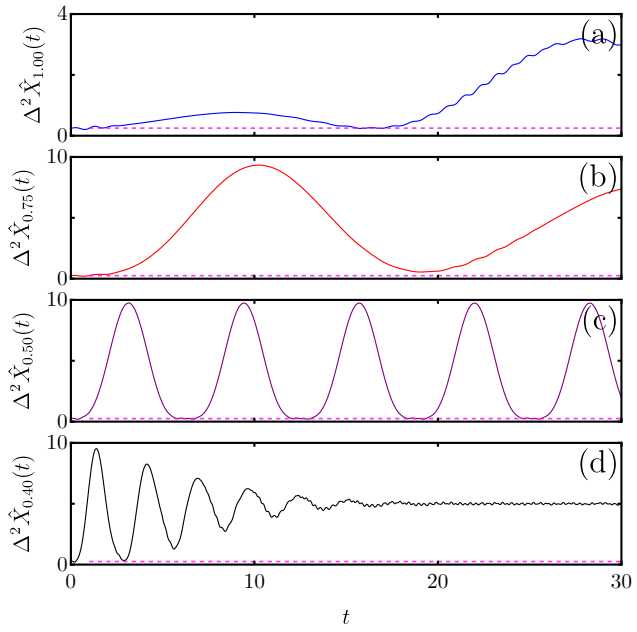

Fig. 4. The quadrature variance for the FTJC model, for different values of α: $\alpha = 1.00$ (a), $\alpha = 0.75$ (b), $\alpha = 0.50$ (c) and $\alpha = 0.40$ (d). The dashed magenta line represents the value $\Delta^2\hat{X}_\alpha(t) = 1/4$.

D. Squeezing

From the combination of the creation and annihilation operators, we define the quadrature operators as

$$\begin{aligned}\hat{X}_\alpha &= \frac{1}{2}(\hat{a} + \hat{a}^\dagger),\\ \hat{Y}_\alpha &= \frac{1}{2i}(\hat{a} - \hat{a}^\dagger),\end{aligned} \tag{18}$$

which correspond to dimensionless analogues of the position and momentum operators, respectively. These operators are canonically conjugate and satisfy the uncertainty relation

$$\Delta^2\hat{X}_\alpha\,\Delta^2\hat{Y}_\alpha \geq \frac{1}{16}. \tag{19}$$

Squeezing occurs when the uncertainty in one of the quadratures is reduced below the standard quantum limit:

$$\Delta^2\hat{X}_\alpha < \frac{1}{4} \quad \text{or} \quad \Delta^2\hat{Y}_\alpha < \frac{1}{4}. \tag{20}$$

Fig. 4 illustrates the variance $\Delta^2\hat{X}_\alpha$ in the fractional-time framework for various values of α. For $\alpha = 1.00$, displayed in panel (a), squeezing is evident during the initial oscillations, followed by an increase in $\Delta^2\hat{X}_{1.00}(t)$. Later, within the interval $10 < t < 20$ and coinciding with the onset of the revival observed in Fig.1(a), non-classical values of the variance reemerge [11]. When $\alpha = 0.75$, squeezing appears only at early times, and the variance attains higher values between the two minima. In contrast, for $\alpha = 0.50$, squeezing occurs periodically at times $t = q\pi$, corresponding to the oscillations seen in Fig. 1(c). At times $t = m\pi$, where even-odd parity shifts are observed in Fig. 2(c), the variance exhibits pronounced peaks. For $\alpha = 0.40$, after initial squeezing and oscillations of diminishing amplitude, the variance approaches an asymptotic value.

E. Husimi Function

The Husimi function, is a non-negative definite distribution that represents the quantum state of light as a quasi-probability function over phase space, employing coherent states as reference points [12]. The Husimi function $\mathcal{Q}_\alpha(t)$ is defined as

$$\mathcal{Q}_\alpha(t) = \frac{1}{\pi}\langle\gamma|\hat{\rho}_\alpha^F(t)|\gamma\rangle, \tag{21}$$

where $|\gamma\rangle$ denotes a coherent state and $\hat{\rho}_\alpha^F(t)$ represents the reduced density matrix of the cavity mode. The latter is obtained by tracing out the atomic degrees of freedom:

$$\hat{\rho}_\alpha^F(t) = \mathrm{Tr}_A\left[\hat{\rho}_\alpha(t)\right], \tag{22}$$

with $\hat{\rho}_\alpha(t) = |\Psi_\alpha(t)\rangle\langle\Psi_\alpha(t)|$ being the density operator of the system.

Fig. 5 displays the Husimi function for various values of α at the time $t = t_r/2 = |\beta|\pi/\mu_\alpha$. Here, t_r denotes the revival time for the standard case $\alpha = 1.00$ [4]. We fix this reference time because, in the conventional scenario, it corresponds to a minimum in entanglement [4], at which point the cavity mode evolves into a Schrödinger cat state. For $\alpha = 1.00$, the Husimi function exhibits a bifurcation into two distinct parts rotating in opposite directions along a circle of radius $|\beta|^2$ centered at the origin [13]. At the specified instant, both parts possess equal intensity but differ in phase, characterizing the formation of the Schrödinger cat state, as illustrated in panel (a). For $\alpha \neq 1.00$, however, the dynamics deviate significantly. The initial distribution splits into two components: one remains at the original position, retaining a Gaussian profile, while the other moves along the circular trajectory of radius $|\beta|^2$. In the case of $\alpha = 0.75$, illustrated in panel (b), the resulting distribution is clearly

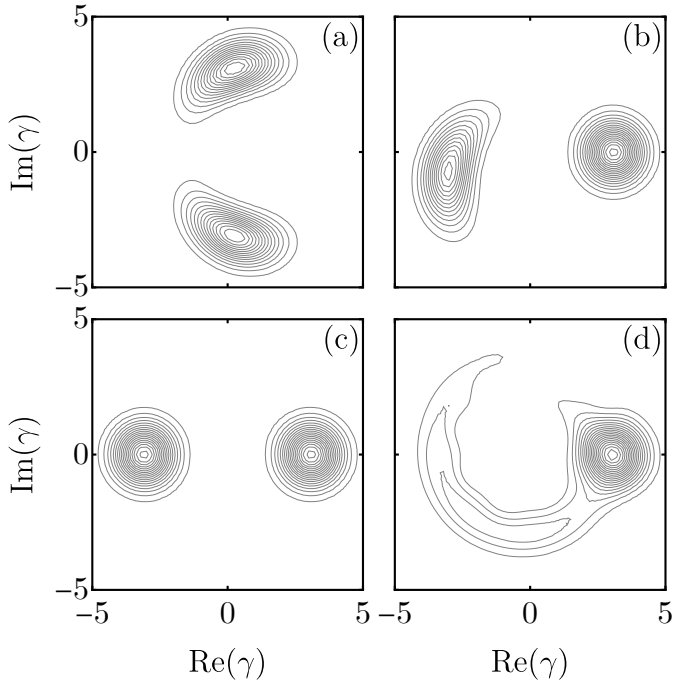

Fig. 5. Husimi function for the FTJC model, for different values of α: $\alpha = 1.00$ (a), $\alpha = 0.75$ (b), $\alpha = 0.50$ (c) and $\alpha = 0.40$ (d).

asymmetric, whereas for $\alpha = 0.50$, shown in panel (c), a cat state re-emerges, this time composed of two Gaussian peaks. Moreover, a connection can be established between the phase-space dynamics and the parity oscillations discussed earlier. In Fig. 5(c), the formation of cat states at times $t = m\pi$ coincides with the even-odd parity transitions seen in Fig. 2(c). For $\alpha = 0.40$, the two components of the Husimi function have merged at the chosen time, though a residual peak remains at the initial point in phase space. A similar merging is observed for $\alpha = 0.75$, albeit at a later time.

Interestingly, the evolution of the Husimi function for $\alpha = 0.50$ bears a resemblance to that of the two-photon JC model with Stark shift [14], although with a slower timescale. In the referenced work, a cat state composed of two Gaussian distributions forms at times $t = m\pi/2$, with $m = 1, 2, \ldots$.

V. Conclusions

In this work, we investigated the unitary dynamics of the FTJC model proposed in Ref. [6], considering the cavity mode initially prepared in a coherent state. We analyzed the photon statistics of the system under different values of the fractional derivative order α, revealing a variety of dynamical behaviors.

For $\alpha = 0.75$, we observed dynamics qualitatively similar to those of the standard JC model, as evidenced by the evolution of the expectation values of the number and parity operators, as well as the Mandel Q-parameter. In contrast, for $\alpha = 0.50$, a clear periodicity emerges across all quantities examined. This regime is marked by enhanced sub-Poissonian statistics and a more pronounced squeezing effect. When $\alpha = 0.40$, the behavior becomes aperiodic, and the quadrature variance asymptotically approaches a constant value. The Husimi quasi-probability distribution further illustrates these trends. Initially, the distribution splits into two components: one remains localized at the origin, while the other rotates along a circular trajectory in phase space. For $\alpha = 0.50$, this configuration persists throughout the time evolution, resulting in the formation of Schrödinger cat states at $t = m\pi$. Notably, the two lobes of the Husimi function acquire Gaussian profiles in this case, resembling the dynamics of the two-photon JC model with Stark shift.

We hope that these findings offer a valuable foundation for future investigations into the physical significance of the FTJC model.

Acknowledgements

We thank Dr. Alison A. da Silva and Dr. Enrique C. Gabrick for helpful discussions.

References

[1] I. Podlubny, *Fractional Differential Equations*. Academic Press, 1998.
[2] C. Zu, Y. Gao, and X. Yu, "Time fractional evolution of a single quantum state and entangled state", *Chaos, Solitons & Fractals*, vol. 147, p. 110930, April 2021.
[3] E. T. Jaynes and F. W. Cummings, 'Comparison of quantum and semiclassical radiation theories with application to the beam maser", *Proceedings of the IEEE*, vol. 51, no. 1, pp. 89–109, January 1963.
[4] J. Larson and T. Mavrogordatos, *The Jaynes–Cummings Model and Its Descendants*. IOP Publishing, Bristol, 2021.
[5] M. Naber, "Time fractional Schrödinger equation", *Journal of Mathematical Physics*, vol. 45, no. 8, pp. 3339–3352, August 2004.
[6] D. Cius, "Unitary description of the Jaynes-Cummings model under fractional-time dynamics", *Physical Review E*, vol. 111, no. 2, pp. 024110, February 2025.
[7] D. Cius, L. Menon, M. A. F. dos Santos, A. S. M. de Castro, and F. M. Andrade, "Unitary evolution for a two-level quantum system in fractional-time scenario", *Physical Review E*, vol. 106, no. 5, p. 054126, November 2022.
[8] A. Iomin, "Fractional time quantum mechanics", in *Volume 5 Applications in Physics, Part B*, edited by V. E. Tarasov, De Gruyter, Berlin and Boston, 2019, pp. 299–316.
[9] A. Fring and M. H. Y. Moussa, "Unitary quantum evolution for time-dependent quasi-Hermitian systems with nonobservable Hamiltonians", *Physical Review A*, vol. 93, no. 4, p. 042114, April 2016.
[10] R. Birrittella, K. Cheng, and C. C. Gerry, "Photon-number parity oscillations in the resonant Jaynes–Cummings model", *Optics Communications*, vol. 354, pp. 286–290, November 2015.
[11] P. Meystre and M. S. Zubairy, "Squeezed states in the Jaynes–Cummings model", *Physics Letters A*, vol. 89, no. 8, pp. 390–392, June 1982.
[12] N. D. Cartwright, "A non-negative Wigner-type distribution", *Physica A: Statistical Mechanics and its Applications*, vol. 83, no. 1, pp. 210–212, 1976.
[13] B. W. Shore and P. L. Knight, "The Jaynes–Cummings model", *Journal of Modern Optics*, vol. 40, no. 7, pp. 1195–1238, July 1993.
[14] V. Bužek and B. Hladký, "Macroscopic superposition states of light via two-photon resonant interaction of atoms with cavity field", *Journal of Modern Optics*, vol. 40, no. 7, pp. 1309–1324, July 1993.